

Determination of key receptor–ligand interactions of dopaminergic arylpiperazines and the dopamine D2 receptor homology model

Vladimir Sukalovic · Vukic Soskic · Milan Sencanski ·
Deana Andric · Sladjana Kostic-Rajacic

Received: 16 October 2012 / Accepted: 11 December 2012 / Published online: 9 January 2013
© Springer-Verlag Berlin Heidelberg 2013

Abstract Interest in structure-based G-protein-coupled receptor (GPCR) ligand discovery is huge, given that almost 30 % of all approved drugs belong to this category of active compounds. The GPCR family includes the dopamine receptor subtype D2 (D2DR), but unfortunately—as is true of most GPCRs—no experimental structures are available for these receptors. In this publication, we present the molecular model of D2DR based on the previously published crystal structure of the dopamine D3 receptor (D3DR). A molecular modeling study using homology modeling and docking simulation provided a rational explanation for the behavior of the arylpiperazine ligand. The observed binding modes and receptor–ligand interactions provided us with fresh clues about how to optimize selectivity for D2DR receptors.

Keywords Dopamine · Molecular modeling · Arylpiperazine · Docking simulations

Electronic supplementary material The online version of this article (doi:10.1007/s00894-012-1731-6) contains supplementary material, which is available to authorized users.

V. Sukalovic (✉) · S. Kostic-Rajacic
ICTM—Centre for Chemistry, University of Belgrade,
Njegoseva 12,
11000 Belgrade, Serbia
e-mail: vladimir.sukalovic@abcsistem.rs

V. Soskic
ORGENTEC Diagnostika GmbH, Carl-Zeiss-Str. 49-51,
Mainz, Germany

M. Sencanski
Innovation Center of the Faculty of Chemistry,
University of Belgrade, Studentski trg 12-16,
11000 Beograd, Serbia

D. Andric
Faculty of Chemistry, University of Belgrade,
Studentski trg 12-16,
11000 Beograd, Serbia

Abbreviations

D2DR Dopamine receptor type 2
ecl Extracellular loop
etf Edge-to-face
D3DR Dopamine receptor type 3

Introduction

G-protein-coupled receptors (GPCRs) are a large family of integral membrane proteins that are a major focus of pharmaceutical research and the primary targets of almost 30 % of all approved drugs [1]. In the human genome, about 360 pharmaceutically relevant GPCRs have been identified, but crystal structures have been determined for only a few of these so far [2].

Since there are so few crystal structures of GPCRs, *in silico* homology models of these receptors could provide templates for the discovery of new receptor ligands. However, this begs the question: how effective are such models in terms of hit rate and affinity compared to the corresponding crystal structures? The answer to that question is provided by the study of Carlsson et al. [1], which showed that a docking screen in which ligands were docked against the homology model of the D3 dopamine (DA) receptor was no less effective than a similar screen in which ligands were docked against the crystal structure. Therefore, homology modeling is required in order to achieve the structure-based discovery of ligands for most GPCRs.

The neurotransmitter dopamine is a major neurotransmitter in the central nervous system (CNS), and plays crucial roles in behavior and cognition. There are five different subtypes of DA receptors, which are classified into two subfamilies (D1-like and D2-like) based on sequence. These are all members of the superfamily of GPCRs, which all have a rhodopsin-like core structure. The D2-like

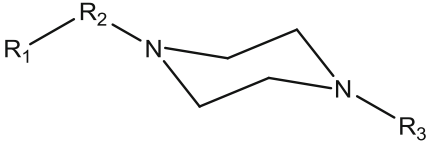
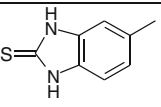
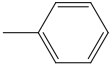
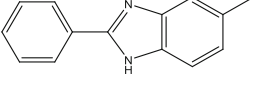
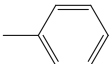
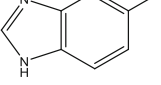
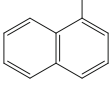
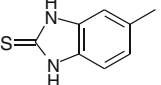
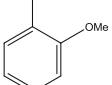
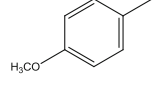
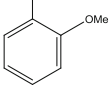
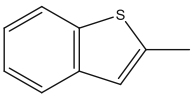
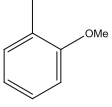
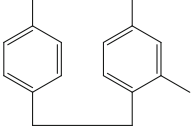
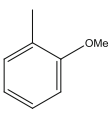
subfamily comprises the D2, D3, and D4 receptors (D2DR, D3DR, and D4DR, respectively). These all share a high degree of sequence identity within the transmembrane (TM) segments, and their near-identity of the residues that form the binding site in these receptors [3] has made it difficult to create subtype-selective agents.

Our research program is focused on the design, synthesis, and testing of new arylpiperazine dopaminergic ligands. Obtaining the 3D structure of the receptor protein would significantly aid our understanding of the molecular mechanism of the receptor–ligand interaction, and would contribute to the drug discovery process. Unfortunately, the 3D structure of the D2 dopamine receptor (D2DR) is not known. Therefore, it was important for us to produce a useful *in silico* molecular model of D2DR.

We used the recently published crystal structure of D3DR [3] as the starting point to construct this *in silico*

3D model of D2DR. The methods of homology modeling were used to construct the initial model. That model was further refined in an iterative process that considered the interactions of a number of known D2DR ligands (Table 1). Special care was taken during the modeling of the extracellular loop (ecl) region of the D2DR model, where the second binding pocket is located [4, 5]. Since the secondary structure of the ecl region is not known, applying homology modeling alone tends to give modest results. Therefore, rather than using existing *in silico* methods alone for ecl modeling, selected D2DR ligands were used as a template. The intracellular loops were initially considered during model construction, but were omitted during subsequent optimization as they do not represent a binding site on D2DR. To demonstrate the usefulness of the new D2DR model, a flexible and partially rigid docking analysis was performed on dopaminergic arylpiperazines, and the results obtained were

Table 1 Arylpiperazine ligands used to construct the D2 DAR model

|  | | | | |
|--|---|---|--|---------------------|
| No | R ₁ | R ₂ | R ₃ | K _i (nM) |
| 1 |  | (CH ₂) ₃ |  | 3.0 |
| 2 |  | (CH ₂) ₂ |  | 60.0 |
| 3 |  | (CH ₂) ₂ |  | 11.3 |
| 4 |  | (CH ₂) ₃ |  | 0.4 |
| 5 |  | -CH=CH-CONH- (CH ₂) ₄ - |  | 12.0 |
| 6 |  | -CONH-(CH ₂) ₄ - |  | 21.0 |
| 7 |  | -CONH-(CH ₂) ₄ - |  | 15.0 |

References: Ligands 1,3,4,5[27], 2[28], 6[29], 7[30]

compared with experimentally obtained ligand–receptor binding data.

Material and methods

Protein modeling

Primary sequence analysis and sequence alignment

The NCBI protein database [6] was searched for the sequence of amino acid residues corresponding to the long form of the human D2DR receptor. The sequence searched for was reported by van Munsterforh D2DR (NP_000786) [7]. The Discovery Studio 2.5 software package [8] was used to align the D2DR sequence with the template protein sequence (see online resource 1 of the “Electronic supplementary material,” ESM).

Prediction and refinement of the 3D structure of D2DR

The modeling of D2DR was carried out using the Discovery Studio 2.5 protein modeling protocol and MODELLER for model building [8]. The model was built using D3DR (PDB code: 3pbl, resolution 2.89 Å) [3] as a template, together with the set of known ligands (Table 1), in order to evaluate the similarity and/or improvement achieved when this structure is employed to generate homology models, as compared to the models obtained using existing templates [9]. The best D2DR model was selected based on the RMSD, and the conformation of the backbone was evaluated in Discovery Studio in order to verify the protein protocol.

Modeling the loop sequences

Discovery Studio was used to model the D2DA receptor loop sequences. The loop sequences were aligned with the D3DR sequence, and this alignment was supplied along with the 3D coordinates of D3DR as an input to the program. Extracellular loops (ecl2 and ecl3) were further refined using Discovery Studio’s loop refinement protocol and a set of ligands (Table 1). A key determinant of the correct orientation of those extracellular loops is the constraint imposed by the positions of the corresponding receptor helices and a disulfide bond between ecl2 and the top of TM domain 3. The Discovery Studio loop refinement protocol modeled the protein loops by attempting to satisfy these restraints.

In order to obtain a relaxed conformation, the generated model was initially subjected to an energy minimization process that involved the use of the conjugate gradient method for about 4,000 iterations, and then to a 2 ns isothermal, constant-volume MD simulation using CHARMM all-hydrogen amino acid parameters, as performed in Discovery Studio.

Explicit membrane simulations

D2DR was inserted into a POPC lipid bilayer of dimensions 80×80 Å using the VMD 1.8.7 program [10]. The system was combined using a tcl script. The ligand was inserted, and oriented towards specific amino acid residues, according to the results obtained from the docking simulations. 25 Å thick water layers were also added on both sides of the z-axis of the system, and the system was neutralized by adding 0.15 M NaCl (assuming physiological conditions). The final number of atoms in the system was 72,726, and the final dimensions of the simulation cell were 86×84×127 Å. The CHARMM22 force field was used for the protein and lipids. The geometry of the ligand was optimized and its Hessian was calculated at the 6-31 G level of theory in Gaussian 03W [11]. The coordinates and Hessian obtained were imported into the Paratool plugin of VMD, where topology and parameter files for the ligand were generated. Partial charges for the ligand atoms were assigned using the 0.9.6 CGenFF force field [12]. The system obtained was set to cascade through 10,000 steps of minimization, 250 ps of equilibration, and 5 ns of production under PBC conditions in the NVT ensemble, as performed using the NAMD 2.7b program [13]. Each integration step was 1 fs. The cutoff was set to 12 Å. After plotting graphs of the potential energy and its derivative, we concluded that system had reached energetic stability (see online resource 2 of the ESM). All calculations were carried out on the PARADOX computer cluster 9e [14].

Ligand construction

The 3D ligand structures were generated using Discovery Studio [8]. As physiological conditions were assumed, the basic aliphatic nitrogen atom of the piperazine was protonated. The geometry was optimized using the CHARMM force field and the conjugate gradient method, which was applied until the energy difference between successive cycles was below 0.0042 kJ/mol.

Model validation

Model validation was performed with a selected set of ligands from the ChEMBL D2DR database [15]. We selected a total of 60 ligands: 30 with a high affinity for D2DR and 30 inactive ligands (see online resource 3 of the ESM). All of the ligands were prepared as described above and docked into the proposed D2DR model.

Docking analysis

For the docking analysis, we used the proposed D2DR model based on the crystal structure of D3DR. The binding

site on the receptor was determined by combining results obtained from experimental data [16, 17] and the Schrödinger Maestro receptor grid generation module [18]. Amino acid residue charges were adjusted where needed, assuming physiological conditions.

Docking of the selected ligands (as presented in Table 3) was performed by the Glide module in Schrödinger Suite 2011 [12]. All ligands were protonated when docked using the OPLS_2005 force field. The initial position of the ligand in the binding site was chosen arbitrarily, while the protonated nitrogen on the ligand part was kept in close proximity to Asp-114 of D2DR. After initial ligand placement, no further constraints were applied, and the docking procedure based on the Glide ligand-docking methodology was carried out. The obtained docked structures were examined, and those with the lowest total docking scores were selected. We selected structures based on the following criteria: best docking score for the complex; shortest salt bridge formed between Asp-114 of D2DR and the proton on the nitrogen; adoption of a chair conformation by the arylpiperazine ring; localization of the aryl part of the molecule in the rear hydrophobic pocket of the receptor (Phe-386, Trp-390, Tyr-420) [19]. After the initial criteria had been satisfied, the second step was to examine the different interactions that can form between receptor and ligand (hydrogen bonds, aromatic–aromatic interactions, etc.). In this way, the best possible docking structures were selected. Structures were visualized using DS Visualize v.2.5.1 [20], and the images obtained were rendered using the POV-Ray raytracer (v.3.6) [21].

Results and discussion

The D2DR model was built in accordance with the notion that the highly homologous D3DR can be adequately used as a template. The major differences between D2DR and D3DR occur in their loops. Therefore, extra care was taken during the modeling of the extracellular loops, since both the second extracellular loop (ecl2) and the third extracellular loop (ecl3) of D2DR are included in the ligand-binding site [22]. Intracellular loop modeling was not considered in this work as these loops do not interact directly with D2DR ligands.

The model obtained was tested using D2DR ligands that have previously been described in the literature (Tables 2 and 3). The model system was subjected to explicit membrane simulations in order to obtain the specific protein–ligand complex conformation and to prove the stability of the assumed interactions. To this end, the system setup was assembled as described before, and the simulation was set to run until completed. During the production phase, the results obtained confirmed the stability of the assumed protein–ligand interactions (Fig. 1).

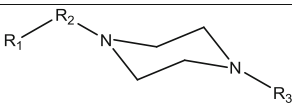
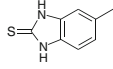
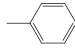
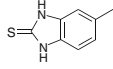
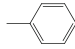
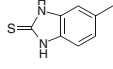
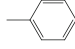
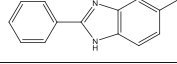
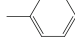
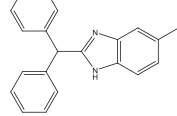
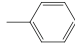
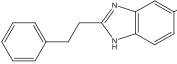
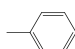
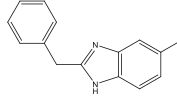
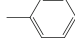
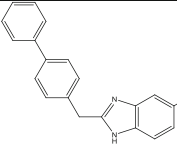
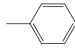
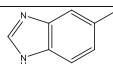
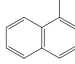
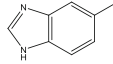
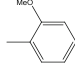
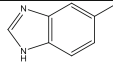
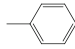
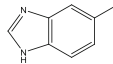
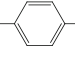
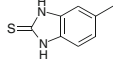
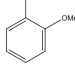
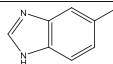
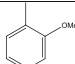
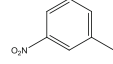
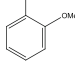
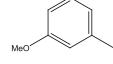
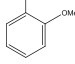
To enhance clarity, the molecular structure of the ligand was divided into three distinct substructure motifs: a fixed piperazine part, a flexible head part, and a flexible linker and tail part (denoted R1, R2, and R3 in Tables 1, 2, and 3).

Model validation was performed using a binary set of ligands (see online resource 3 of the ESM). Active ligands were selected with a particular minimal arylpiperazine structure in mind, whereas inactive ligands were picked at random. A total of 60 ligands were submitted to docking analysis. Two sets of rules were applied to filter the docked ligands. First, the arylpiperazine part of the ligand had to be positioned in the orthosteric binding site (OBS) of the receptor (there had to be a short salt bridge between Asp-114 and the protonated nitrogen atom of the ligand, at least one hydrogen bond between the ligand and Ser-167, Ser-194, or Ser-197 [5], and there had to be hydrophobic interactions of the tail end of the ligand with Phe-386, Trp-390, and Tyr-420 [4]). Second, ligands with large hydrophobic groups in the head part of the molecule should dock into the second binding pocket (SBP), located in the ecl part of D2DR. All 30 active ligands docked in the correct position (see online resource 4 of the ESM), while the inactive ones failed to produce any logical structure.

The next step was to perform a docking analysis of the series of test ligands. These ligands were divided into several groups in order to test the different aspects of the receptor–ligand interactions (Table 2) that the new D2DR model had to address. The first group (ligands 8–10) had different linker lengths. Increasing the length of the linker from one to three $-\text{CH}_2-$ groups led to an increase in affinity, with ligand 10 having the highest affinity. The second group (ligands 11–15) had different head parts. The head part varied in both length and size. Ligands 11–14 were found to bind to D2DR, whereas compound 15 did not, due to its length. The third group of ligands (16–19) had different tail parts, and included high-affinity ligands (16 and 17) and a compound (19) that could not bind due to its length. The fourth group of ligands (20–23) also had different head parts. Ligands 20 and 21 differed in their potential for hydrogen-bond formation, while ligands 22 and 23 yielded the correct binding site receptor–ligand orientation, as the head part was similar to the tail part in each ligand.

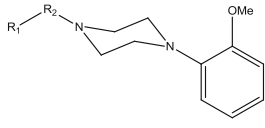
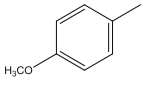
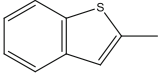
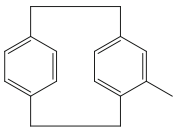
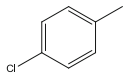
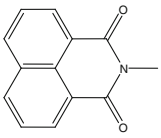
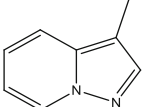
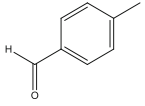
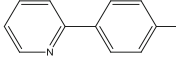
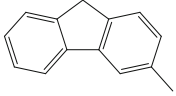
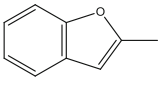
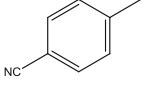
The receptor binding site was defined based on experimental and literature data [23]. Glide Receptor grid generation was performed under the following constraints: the protonated nitrogen atom on the ligand had to be in close proximity to Asp-114; the ligand was able to form hydrogen bonds with Ser-167, Ser-194, or Ser-197; two hydrophobic pockets were present—one in OBS (formed by Phe-386, Trp-390, and Tyr-420), and the other in the SBP (ecl2 area; formed by Ile-166, Leu-170, Leu-171, Ile-184, Phe-189, Val-190, His-397, and Ile-398). Docking results were visualized in a schematic representation (Fig. 2).

Table 2 Arylpiperazine ligands used to test the D2DR model

|  | | | | | |
|---|---|---------------------------------|---|------------------------|---|
| No | R ₁ | R ₂ | R ₃ | K _i (nM) | Docking score (kcal mol ⁻¹) |
| 8 |  | CH ₂ |  | >1000 | -6.7 |
| 9 |  | (CH ₂) ₂ |  | 15.7 | -10.7 |
| 10 |  | (CH ₂) ₃ |  | 3.0 | -12.5 |
| 11 |  | (CH ₂) ₂ |  | 60.2 | -10.66 |
| 12 |  | (CH ₂) ₂ |  | 76.3 | -9.39 |
| 13 |  | (CH ₂) ₂ |  | 117.0 | -8.11 |
| 14 |  | (CH ₂) ₂ |  | 157.0 | -5.87 |
| 15 |  | (CH ₂) ₂ |  | >1000 | n/a |
| 16 |  | (CH ₂) ₂ |  | 11.3 | -10.22 |
| 17 |  | (CH ₂) ₂ |  | 13.3 | -10.14 |
| 18 |  | (CH ₂) ₂ |  | 138.0 | -6.73 |
| 19 |  | (CH ₂) ₂ |  | >1000 | n/a |
| 20 |  | (CH ₂) ₃ |  | 0.4 | -10.62 |
| 21 |  | (CH ₂) ₃ |  | 97.0 | -8.19 |
| 22 |  | -CH=CHCH ₂ - |  | 16.9 | -9.35 |
| 23 |  | -CH=CHCH ₂ - |  | 36.0 | -8.35 |

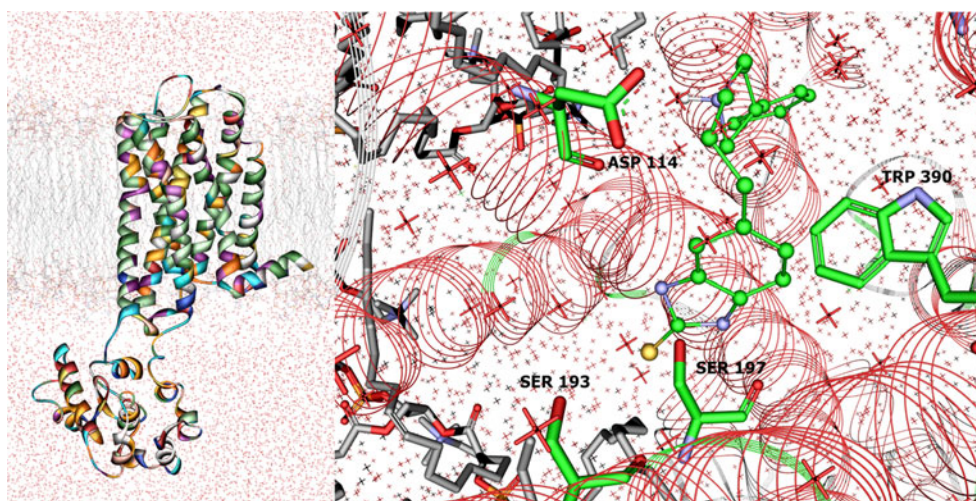
References: Ligands 8–23[31]

Table 3 Ligands used to probe the ec12 area of the D2DR model

|  | | | | |
|---|---|---|---------|---|
| No | R ₁ | R ₂ | Ki (nM) | Docking score (kcal mol ⁻¹) |
| 24 |  | -CH=CH-CONH-(CH ₂) ₄ - | 12.0 | -7.6 |
| 25 |  | -CONH-(CH ₂) ₄ - | 21.0 | -9.9 |
| 26 |  | -CONH-(CH ₂) ₄ - | 15.0 | -12.2 |
| 27 |  | -CONH-(CH ₂) ₄ - | 19.0 | -6.8 |
| 28 |  | -(CH ₂) ₄ - | 40.0 | -11.6 |
| 29 |  | -CONH-(CH ₂) ₃ - | 11.0 | -9.6 |
| 30 |  | -CH=CH-CONH-(CH ₂) ₄ - | 11.0 | -8.3 |
| 31 |  | -CONH-(CH ₂) ₄ - | 28.0 | -8.1 |
| 32 |  | -CONH-CH ₂ CH=CHCH ₂ - | 48.0 | -8.9 |
| 33 |  | -CONH-(CH ₂) ₄ - | 36.0 | -8.3 |
| 34 |  | -CH=CH-CONH-(CH ₂) ₄ - | 10.0 | -11.2 |

References: Ligands 24,27,28,30,34[32], 25[29], 26[30], 29[33], 31,32[34], 33[29]

Fig. 1 Results of the explicit membrane simulations. *Left*: dopamine D2 receptor model in a lipid bilayer; *right*: part of the receptor with ligand 10 in the binding site



In addition to the protonated nitrogen atom that forms a salt bridge with Asp-114, which is crucial to the binding of the ligand to D2DR, we observed a number of other key interactions that contribute to high ligand affinity. Those

interactions are a hydrogen bond between the ligand and Ser-194, Ser-197, or Ser-167, and aromatic interactions (most probably of edge-to-face type) between the tail part of the ligand and Phe-386, Trp-390, and Tyr-420 of the

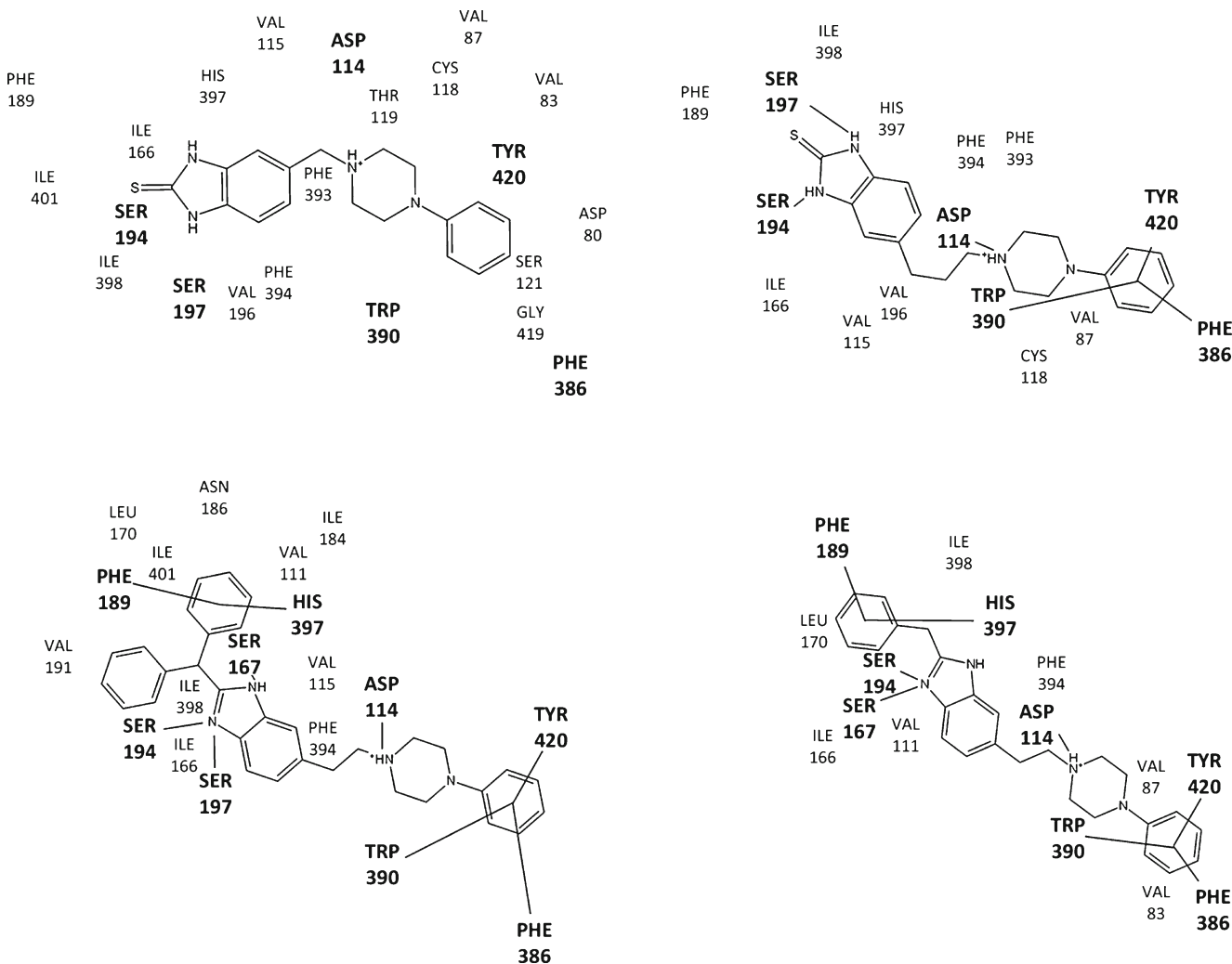


Fig. 2 Docking schematic results for ligands 8 (*upper left*), 10 (*upper right*), 11 (*lower left*), and 14 (*lower right*)

receptor (the OBS pocket). Ligands 8–10 bind to D2DR with the tail part fitting into the hydrophobic pocket and the head part responsible for hydrogen-bond formation with the serine residues listed above. An appropriate linker length is crucial to optimal hydrogen-bond formation, and the docking score reflects that fact. Ligand 10 has the best docking score and the highest D2DR affinity (see Fig. 2 and online resource 5 in the ESM).

Explicit membrane simulations performed with ligand 10 showed that the protein–ligand complex was stable, confirming the results obtained from molecular docking. During the production phase, the salt bridge between the protonated nitrogen of the ligand and Asp-114 remained stable. Hydrogen bonds formed between Ser-194 and the head of the ligand (preferably via the sulfur atom rather than the nitrogen; see online resources 6 and 7 of the ESM), and a hydrogen bond formed between the ring nitrogen and Ser-197.

Ligands 11–15 were found to bind in a similar manner. A salt bridge was formed with Asp-114, the tail segment was observed to bind into a hydrophobic pocket, while the head segment formed hydrogen bonds with Ser-167, Ser-194, or Ser-197. The aromatic part of the head segment was able to bind into another hydrophobic pocket (the SBP) formed by amino acid residues of ecl2 and ecl3. Ligands 11–14 formed aromatic (or hydrophobic) interactions with Ile-166, Leu-170, Leu-171, Ile-184, Phe-189, Val-190, His-397, and Ile-398, located in the SBP (Fig. 2). Since the loop segments of the receptor lack a definitive structure, the rigid ligands 11 and 12 had slightly higher affinities than the more flexible ligands 13 and 14. Ligand 15 was not able to bind, due to its size. The docking scores obtained follow the trend in ligand affinity.

Ligands 16–19 have different tail segments. These tail segments were seen to bind into OBP and interact with Phe-386, Trp-390, and Tyr-420. Ligand 16 formed multiple edge-to-face interactions, and its size and shape account for its high affinity. Besides those edge-to-face interactions, ligand 17 formed a hydrogen bond with Tyr-420. This combination of hydrogen bond and edge-to-face interactions led to another high-affinity ligand. Ligand 18 is smaller than 16 and thus has less area to form edge-to-face interactions, so it showed lower affinity than 16. Ligand 19 did not bind to D2DR, due to its size. The proximity of the bulk to position 4 of the aromatic tail part was not tolerated due to a steric clash with Phe-368 [24]. Again, the proposed D2DR model differentiated between docked ligands. The docking score reflects experimental data, and the docking results can explain those findings.

Ligands 20–23 were observed to bind in a similar manner to that described above. For ligand 20, the head part formed multiple hydrogen bonds with serine residues of the SBP (Ser-167, Ser-194, or Ser-194). The linker was long enough

to localize the head part an optimal distance from the serine residues, while the tail part formed a hydrogen bond with Tyr-420 and edge-to-face interactions with Phe-386 and Trp-390 in OBP. All of these interactions led to a high affinity of 0.4 nM. Ligand 21 has a different head part to ligand 20; it formed one hydrogen bond less and showed a reduced D2DR affinity compared to 20. Ligands 22 and 23 were docked to test if the proposed D2DR model was able to differentiate between the tail and head parts of the ligand when there were similar aromatic moieties. Docking results showed that both of these ligands docked into the receptor with the correct orientation (see online resources 8 and 9 of the ESM).

The main feature of the D2DR model presented here is its structured extracellular loop area (Fig. 3). As we mentioned before, ecl2 folds down onto the receptor-binding cavity and, together with part of ecl3, forms a “lid” on the D2DR binding site [19]. This part of D2DR was examined in some detail using an amino acid point mutation approach [16], and a number of key amino acid residues that are important for interactions were identified. In our approach, we started from the published D3DR ecl template, and then performed a loop-refining procedure [7]. Further optimization was performed through an interactive process in which known ligands were docked into the initial model. The selected ligands (Table 3) had the same tail and similar linker parts, while the head part was varied to account for all possible interactions with the receptor (aromatic interactions, polar interactions, and hydrogen bonds). To test the D2DR model obtained, a total of 11 ligands (Table 3) were docked using induced-fit docking to account for the flexibility of the amino acid residues in the extracellular loop region of the receptor.

The docking results show that all docked ligands bind to D2DR in a similar manner (Fig. 3). A short salt bridge with Asp-114, a hydrogen bond with Ser-194 or Ser-197, and multiple interactions with Phe-386, Trp-390, and Tyr-420 are all present. Also, the tail parts of the ligands fit well into the SBP area formed by ecl2 and part of ecl3. The docking analysis results shown in Fig. 4 and in online resource 10 of the ESM highlight a number of amino acid residues that are responsible for receptor–ligand interactions. Most prominent are Phe-189 on ecl2 and His-397 bordering the helical structure and ecl3. Those two amino acid residues are found in almost all of the docking results to participate in receptor–ligand interactions. In the case of Phe-189, these interactions are aromatic (edge-to-face), while His-397 can form either aromatic (edge-to-face) interactions or sometimes a hydrogen bond, depending on the structure of the ligand. Besides those two residues, a number of other amino acid residues play important roles by forming a hydrophobic binding pocket in the loop region of the receptor. These residues are: Ile-166, Leu-170, Leu-171, Ile-184, Val-190, and Ile-

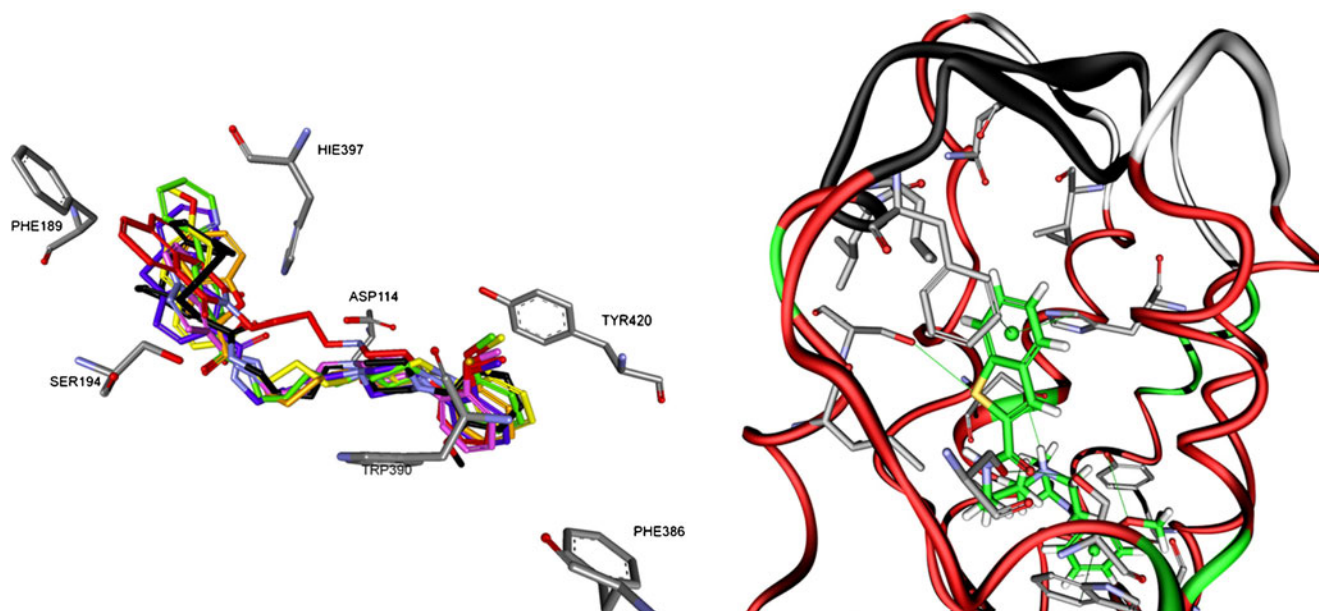


Fig. 3 *Left:* ligands 24, 26, 28, 31, and 33 (overlaid) docked into the 3D model of D2DR. *Right:* ligand 25 positioned inside the receptor binding site. Only key amino acid residues are shown; ecl2 is shown in *black*

398. They participate in hydrophobic or $-\text{CH}-\pi$ interactions, depending on the structure of the ligand (Fig. 4). Another amino acid located in SBP that plays an important role in binding ligands is Asn-186. This residue can engage in polar interactions or a hydrogen bond with a ligand that has a compatible structure (Fig. 4).

To validate the model of D2DR obtained in this work, we studied the docking of 11 ligands that have distinctive structural features, as follows. Ligands 26, 31, and 32 can only form aromatic interactions (aromatic–aromatic interactions, hydrophobic interactions, and edge-to-face interactions) with Ile-166, Leu-170, Leu-171, Ile-184, Phe-189, Val-190, His-397, and Ile-398. In addition to those interactions, ligands 25, 28, 29, and 33 can form an additional hydrogen bond with His-397, and ligands 24, 27, 30, and 34 can form additional hydrogen bonds with His-397 and Asn-186.

A ligand-binding pocket located between TM 3, 5, 6, and 7 has been identified in many GPCR systems by mutagenesis studies [17, 19, 25]. The presence of such a ligand-binding pocket has come to be regarded as a common feature throughout the entire class A GPCR family. Within the OBS, residues toward the lower part of the pocket tend to be more conserved (Phe or Tyr in 91 and 98 % of the receptors, respectively, and Trp in 90 % of the receptors) [26].

Although all of the ligands orientated correctly in the binding pocket of D2DR, the docking scores obtained for the 11 ligands failed to show any meaningful correlation with ligand activity. When the docking scores of structurally similar ligands were compared, the correlation with ligand

activity increased. For example, ligands 24, 27, 30, and 34 yield $r=0.72$, while ligands 25, 29, 31, and 33 yield $r=0.78$. Ligands 26, 28, and 32 decrease the correlation when they are included in ligand docking score comparisons. Thus, while there are trends in ligand activity and docking score for each group of structurally similar ligands, there is no correlation across the whole series. One possible explanation for these results could be a limited capacity of the docking software to fully account for aromatic interactions, since the activities of all the docked ligands depend on aromatic interactions to some degree. Even though OPLS-2005 performs reasonably well, there are significant limitations to its accuracy when dealing with ETF interactions, which might have significantly influenced the docking scores obtained here.

Conclusions

The model described in this study can explain the binding properties of different arylpiperazine classes of ligands to D2DR, so it should be very useful in virtual screening studies.

The D2DR model was constructed using a number of different ligands that all have an arylpiperazine moiety in common. This model had to include a number of common interactions between ligands and receptors in the OBS and SBP.

Key amino acid residues located in the OBS of the receptor that are essential for arylpiperazine binding are: Asp-114, Ser-167, Ser-194, Ser-197, Phe-386, Trp-390, and Tyr-420.

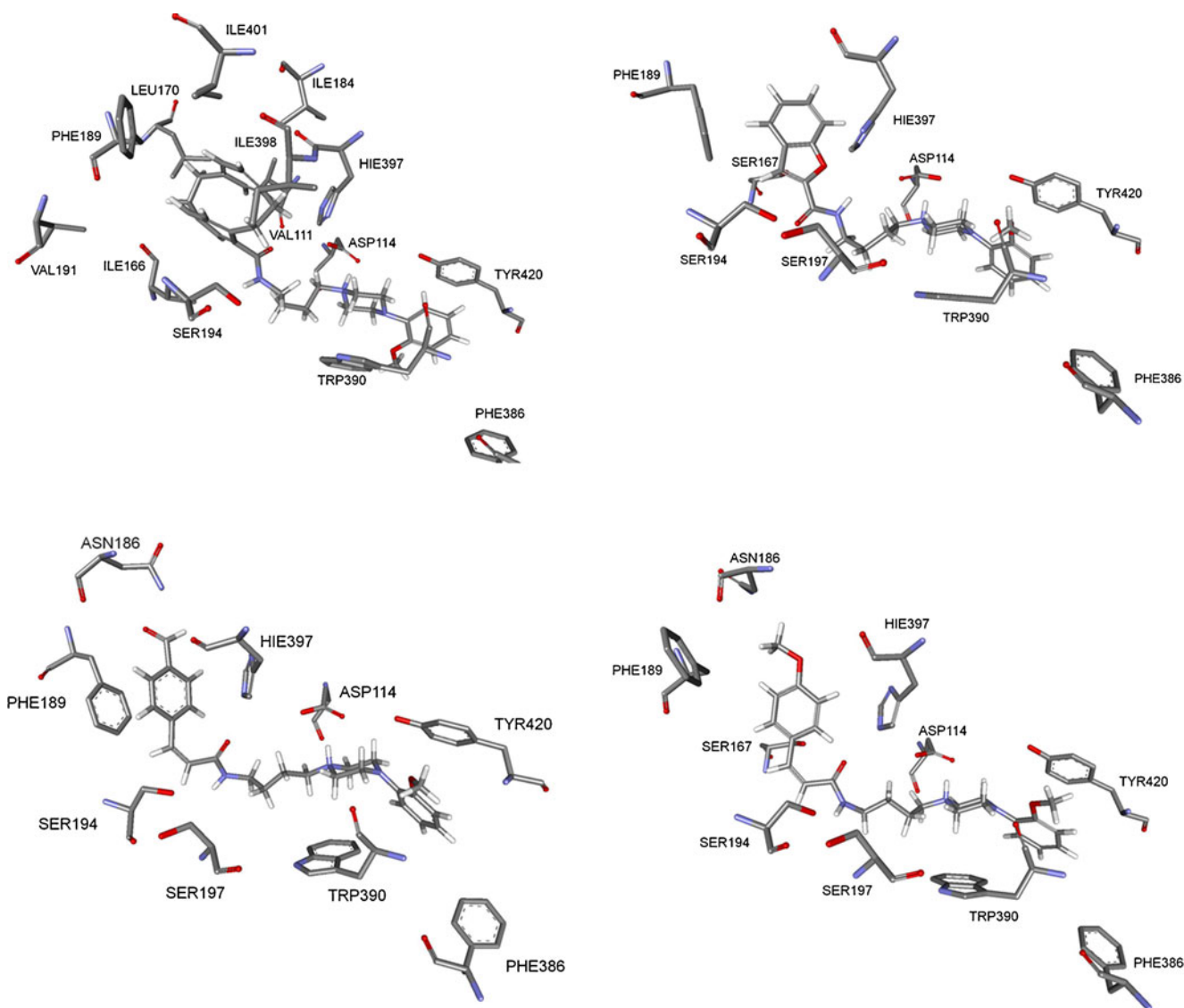


Fig. 4 Docking results for ligands 24 (lower left), 26 (upper left), 30 (lower right), and 33 (upper right)

The high-resolution structure of bovine rhodopsin revealed that *ec12* folds down into the transmembrane domain and forms part of the ligand-binding surface for retinal. Whether *ec12* plays a related role in other rhodopsin-like GPCRs is unclear [22]. Key amino acid residues essential for arylpiperazine binding that are located in *ec12* (SBP) are Ile-166, Leu-170, Leu-171, Ile-184, Phe-189, Val-190, His-397, and Ile-398, and Asn-186 is involved in polar interactions. These findings are consistent with results obtained by Shi and Javitch, who used site-directed mutagenesis to systematically identify residues in *ec12* of D2DR that contribute to the binding-site crevice [22]. Aromatic interactions are most likely of edge-to-face type with Phe-189 or CH- π (or NH- π) interactions with His-397. A polar interaction with Asn-186 may also be responsible for the high binding affinities of ligands with corresponding functional groups. The

size of the ligand is important. Short ligands will not benefit from interactions with SBP, while long ligands will suffer from steric interactions with amino acid residues in the loop. The head part of the ligand should have at least one aromatic ring, but systems with two or more aromatic rings are well tolerated unless the maximum length permitted for the ligand is reached. High affinity can be achieved through aromatic interactions alone or together with polar interactions. Ligands with halogen atoms or polar groups have affinities that are comparable to those of their aromatic analogs. The linker part of the ligand should be as flexible as possible, since this allows optimum positioning of the head part into the SBP formed by *ec12*.

In order to verify the proposed D2DR model, further work on the target-driven synthesis of the new ligand that can distinguish between the proposed molecular interactions

is necessary. The final goal is to obtain a workable D2DR model that will facilitate the design of new specific dopaminergic drugs.

Acknowledgments This research formed part of project 172032 funded by the Ministry of Education and Science, Republic of Serbia.

PARADOX cluster at the Scientific Computing Laboratory of the Institute of Physics Belgrade, is supported in part by the Serbian Ministry of Education and Science under project no. ON171017, and by the European Commission under FP7 projects HP-SEE, PRACE-IIP, PRACE-2IP, EGI-INSPIRE.

References

- Carlsson J, Coleman RG, Setola V, Irwin JJ, Fan H, Schlessinger A, Sali A, Roth BL, Shoichet BK (2011) Ligand discovery from a dopamine D3 receptor homology model and crystal structure. *Nat Chem Biol* 7(11):769–778
- Filizola M, Devi LA (2012) Structural biology: how opioid drugs bind to receptors. *Nature* 485(7398):314–317
- Chien EY, Liu W, Zhao Q, Katritch V, Han GW, Hanson MA, Shi L, Newman AH, Javitch JA, Cherezov V, Stevens RC (2010) Structure of the human dopamine D3 receptor in complex with a D2/D3 selective antagonist. *Science* 330:1091–1095
- Sukalovic V, Ignjatovic D, Tovilovic G, Andric D, Shakib K, Kostic-Rajacic S, Soskic V (2012) Interactions of N-{[2-(4-phenyl-piperazin-1-yl)-ethyl]-phenyl}-2-aryl-2-yl-acetamides and 1-{[2-(4-phenyl-piperazin-1-yl)-ethyl]-phenyl}-3-aryl-2-yl-ureas with dopamine D2 and 5-hydroxytryptamine 5HT(1A) receptors. *Bioorg Med Chem Lett* 22(12):3967–3972
- Newman AH, Beuming T, Banala AK, Donthamsetti P, Pongetti K, Labounty A, Levy B, Cao J, Michino M, Luedtke RR, Javitch JA, Shi L (2012) Molecular determinants of selectivity and efficacy at the dopamine D3 receptor. *J Med Chem* 55(15):6689–6699
- National Center for Biotechnology Information (2012) The National Center for Biotechnology Information advances science and health database. <http://www.ncbi.nlm.nih.gov/protein>. Accessed 27 Dec 2012
- Van Munster BC, de Rooij SE, Yazdanpanah M, Tienari PJ, Pitkala KH, Osse RJ, Adamis D, Smit O, van der Steen MS, van Houten M, Rahkonen T, Sulkava R, Laurila JV, Strandberg TE, Tulen JH, Zwang L, MacDonald AJ, Treloar A, Sijbrands EJ, Zwinderman AH, Korevaar JC (2010) The association of the dopamine transporter gene and the dopamine receptor 2 gene with delirium, a meta-analysis. *Am J Med Genet B Neuropsychiatr Genet* 153B(2):648–655
- Accelrys Software Inc. (2009) Discovery Studio Modeling Environment, release 2.5. Accelrys Software Inc., San Diego
- Teeter MM, Froimowitz M, Stec B, DuRand CJ (1994) Homology modeling of the dopamine D2 receptor and its testing by docking of agonists and tricyclic antagonists. *J Med Chem* 37(18):2874–2888
- Humphrey W, Dalke A, Schulten K (1996) VMD—visual molecular dynamics. *J Molec Graph* 14:33
- Frisch MJ, Trucks GW, Schlegel HB, Scuseria GE, Robb MA, Cheeseman JR, Montgomery JA Jr, Vreven T, Kudin KN, Burant JC, Millam JM, Iyengar SS, Tomasi J, Barone V, Mennucci B, Cossi M, Scalmani G, Rega N, Petersson GA, Nakatsuji H, Hada M, Ehara M, Toyota K, Fukuda R, Hasegawa J, Ishida M, Nakajima T, Honda Y, Kitao O, Nakai H, Klene M, Li X, Knox JE, Hratchian HP, Cross JB, Bakken V, Adamo C, Jaramillo J, Gomperts R, Stratmann RE, Yazyev O, Austin AJ, Cammi R, Pomelli C, Ochterski JW, Ayala PY, Morokuma K, Voth GA, Salvador P, Dannenberg JJ, Zakrzewski VG, Dapprich S, Daniels AD, Strain MC, Farkas O, Malick DK, Rabuck AD, Raghavachari K, Foresman JB, Ortiz JV, Cui Q, Baboul AG, Clifford S, Cioslowski J, Stefanov BB, Liu G, Liashenko A, Piskorz P, Komaromi I, Martin RL, Fox DJ, Keith T, Al-Laham MA, Peng CY, Nanayakkara A, Challacombe M, Gill PMW, Johnson B, Chen W, Wong MW, Gonzalez C, Pople JA (2004) Gaussian 03, revision E.01. Gaussian, Inc., Wallingford
- Vanommeslaeghe K, Hatcher E, Acharya C, Kundu S, Zhong S, Shim J, Darian E, Guvench O, Lopes P, Vorobyov I, MacKerell AD Jr (2010) CHARMM general force field: a force field for drug-like molecules compatible with the CHARMM all-atom additive biological force field. *J Comput Chem* 31:671–690
- Phillips JC, Braun R, Wang W, Gumbart J, Tajkhorshid E, Villa E, Chipot C, Skeel RD, Kale L, Schulten K (2005) Scalable molecular dynamics with NAMD. *J Comput Chem* 26:1781–1802
- PARADOX cluster at the Scientific Computing Laboratory of the Institute of Physics Belgrade <http://www.scl.rs/>. Accessed 27 Dec 2012
- European Bioinformatics Institute <https://www.ebi.ac.uk/chembl/db/target/results/1/compounds/desc/tab/classification>. Accessed 27 Dec 2012
- Javitch JA (1998) Mapping the binding-site crevice of the D2 receptor. *Adv Pharmacol* 42:412–415
- Javitch JA, Fu D, Chen J, Karlin A (1995) Mapping the binding-site crevice of the dopamine D2 receptor by the substituted-cysteine accessibility method. *Neuron* 14(4):825–831
- Schrödinger, LLC (2011) Glide, version 5.7. Schrödinger, LLC, New York
- Javitch JA, Ballesteros JA, Weinstein H, Chen J (1998) A cluster of aromatic residues in the sixth membrane-spanning segment of the dopamine D2 receptor is accessible in the binding-site crevice. *Biochemistry* 37(4):998–1006
- Accelrys Software Inc. (2009) Discovery Studio Modeling environment, release 2.5: Discovery Studio Visualiser 2.5.1. Accelrys Software Inc., San Diego
- Persistence of Vision Raytracer Ltd. (2003–2007) Persistence of Vision Raytracer (POV-Ray). <http://www.povray.org/>
- Shi L, Javitch JA (2004) The second extracellular loop of the dopamine D2 receptor lines the binding-site crevice. *Proc Natl Acad Sci USA* 101(2):440–445
- Sukalovic V, Zlatovic M, Andric D, Roglic G, Kostic-Rajacic S, Soskic V (2004) Modeling of the D2 dopamine receptor arylpiperazine binding site for 1-[2-[5-(1H-benzimidazole-2-thione)]ethyl]-4-aryl piperazines. *Arch Pharm (Weinheim)* 337(9):502–512
- Sukalovic V, Zlatovic M, Andric D, Roglic G, Kostic-Rajacic S, Soskic V (2005) Interaction of arylpiperazines with the dopamine receptor D2 binding site. *Arzneimittelforschung* 55(3):145–152
- Gloriam E, Foord M, Blaney E, Garland L (2009) Definition of the G protein-coupled receptor transmembrane bundle binding pocket and calculation of receptor similarities for drug design. *J Med Chem* 52(14):4429–4442
- Bondensgaard K, Ankersen M, Thøgersen H, Hansen B, Wulff B, Bywater R (2004) Recognition of privileged structures by G-protein coupled receptors. *J Med Chem* 47(4):888–899
- Dukic S, Vujovic M, Soskic V, Joksimovic J (1997) Structure–affinity relationship studies on D-2/5-HT1A receptor ligands. 4-(2-Heteroarylethyl)-1-aryl piperazines. *Arzneimittelforschung* 47(3):239–243
- Kostic-Rajacic S, Soskic V, Joksimovic J (1998) Mixed dopaminergic/serotonergic properties of several 2-substituted 4-[2-(5-benzimidazole)ethyl]-1-aryl piperazines. *Arch Pharm (Weinheim)* 331(1):22–26
- Newman AH, Grundt P, Cyriac G, Deschamps JR, Taylor M, Kumar R, Ho D, Luedtke RR (2009) N-(4-(4-(2,3-dichloro- or 2-methoxyphenyl)piperazin-1-yl)butyl)heterobiarylcarboxamides

- with functionalized linking chains as high affinity and enantioselective D3 receptor antagonists. *J Med Chem* 52(8):2559–2570
30. Schlotter K, Boeckler F, Hubner H, Gmeiner P (2005) Fancy bioisosteres: metallocene-derived G-protein-coupled receptor ligands with subnanomolar binding affinity and novel selectivity profiles. *J Med Chem* 48(11):3696–3699
31. Soskic V, Dukic S, Dragovic D, Joksimovic J (1996) Synthesis of *N*-*n*-propyl-*N*-(2-arylethyl)-5-(1H-benzimidazol-2-thione)-ethylamines and related compounds as potential dopaminergic ligands. *Arzneimittelforschung* 46(8):741–746
32. Hackling A, Ghosh R, Perachon S, Mann A, Holtje HD, Wermuth CG, Schwartz JC, Sippl W, Sokoloff P, Stark H (2003) *N*-(omega-(4-(2-methoxyphenyl)piperazin-1-yl)alkyl)carboxamides as dopamine D2 and D3 receptor ligands. *J Med Chem* 46(18):3883–3899
33. Ehrlich K, Gotz A, Bollinger S, Tschammer N, Bettinetti L, Harterich S, Hubner H, Lanig H, Gmeiner P (2009) Dopamine D2, D3, and D4 selective phenylpiperazines as molecular probes to explore the origins of subtype specific receptor binding. *J Med Chem* 52(15):4923–4935
34. Grundt P, Carlson EE, Cao J, Bennett CJ, McElveen E, Taylor M, Luedtke RR, Newman AH (2005) Novel heterocyclic trans olefin analogues of *N*-{4-[4-(2,3-dichlorophenyl)piperazin-1-yl]butyl} arylcarboxamides as selective probes with high affinity for the dopamine D3 receptor. *J Med Chem* 48(3):839–848